Energetics of the Time-Dependent Natural Orbitals of Molecules

Hirohiko Kono[1], Tsuyoshi Kato[2] ,Takayuki Oyamada[1] ,Shiro Koseki[3]

1. Tohoku Univ. 2. Univ. of Tokyo 3. Osaka Prefectural Univ.

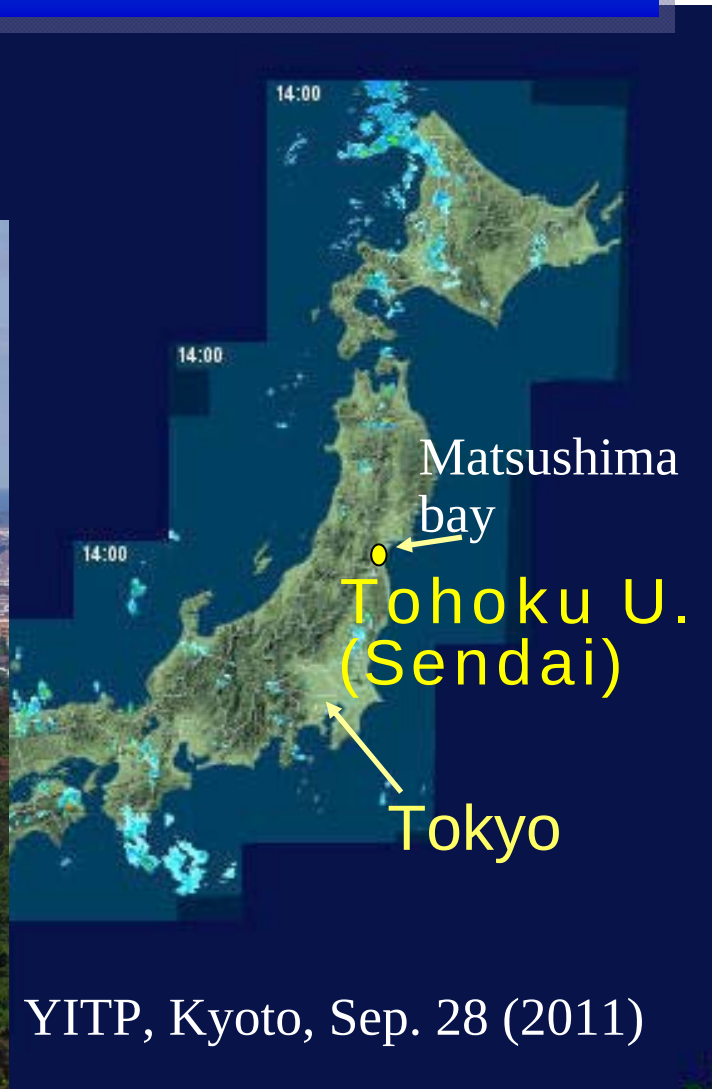

YITP, Kyoto, Sep. 28 (2011)

Interaction of molecules with fs laser pulses

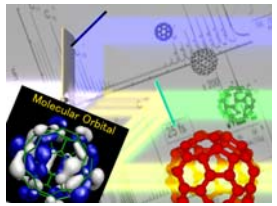

(1) Radiative interaction: One-body interaction (fs or as regime)

An electron or electrons get energy → Energy sharing by many electrons

Development of MCTDHF in grid space

T. Kato and H. Kono
J. Chem. Phys. **128**, 184102 (2008);
Chem. Phys. **366**, 46 (2009).

Characterization of multi-electron dynamics by "time-dependent" chemical potential

- Classification of adiabatic or nonadiabatic processes
- Quantification of energy exchange between molecular orbitals

(2) Energy transfer to vibrational degrees of freedom (10-100 fs)

Coupling of laser-induced ultrafast
π-electron rotations with vibrational modes
in chiral aromatic molecules

M. Kanno, H. Kono, Y. Fujimura,
and S. H. Lin
Phys. Rev. Lett. **104**, 108302 (2010).

(3) Intramolecular Vibrational Energy Redistribution (IVR)
among different vibrational modes (1 ps –)
→Rearrangement or reaction processes (ps –ns)

Difficulties in the control of big molecules such as C_{60}; fast IVR

How to overcome:

e.g., Initial mode selective vibrational excitation by intense near-IR pulses > IVR

Ultrashort “Intense” Laser Pulses

Pulse length → femoto-second (10^{-15} s)

Attosecond (10^{-18} s)

Light intensity → $\sim 10^{20}$ W/cm^2

Hydrogen atom

Electron

Bohr period=24 as

Bohr radius

Atomic Units

Electric field F=5.1x10^9 V/cm

Proton

Light Intensity I=3.5x10^{16} W/cm^2

Tunnel Ionization of H atom in a near-IR field

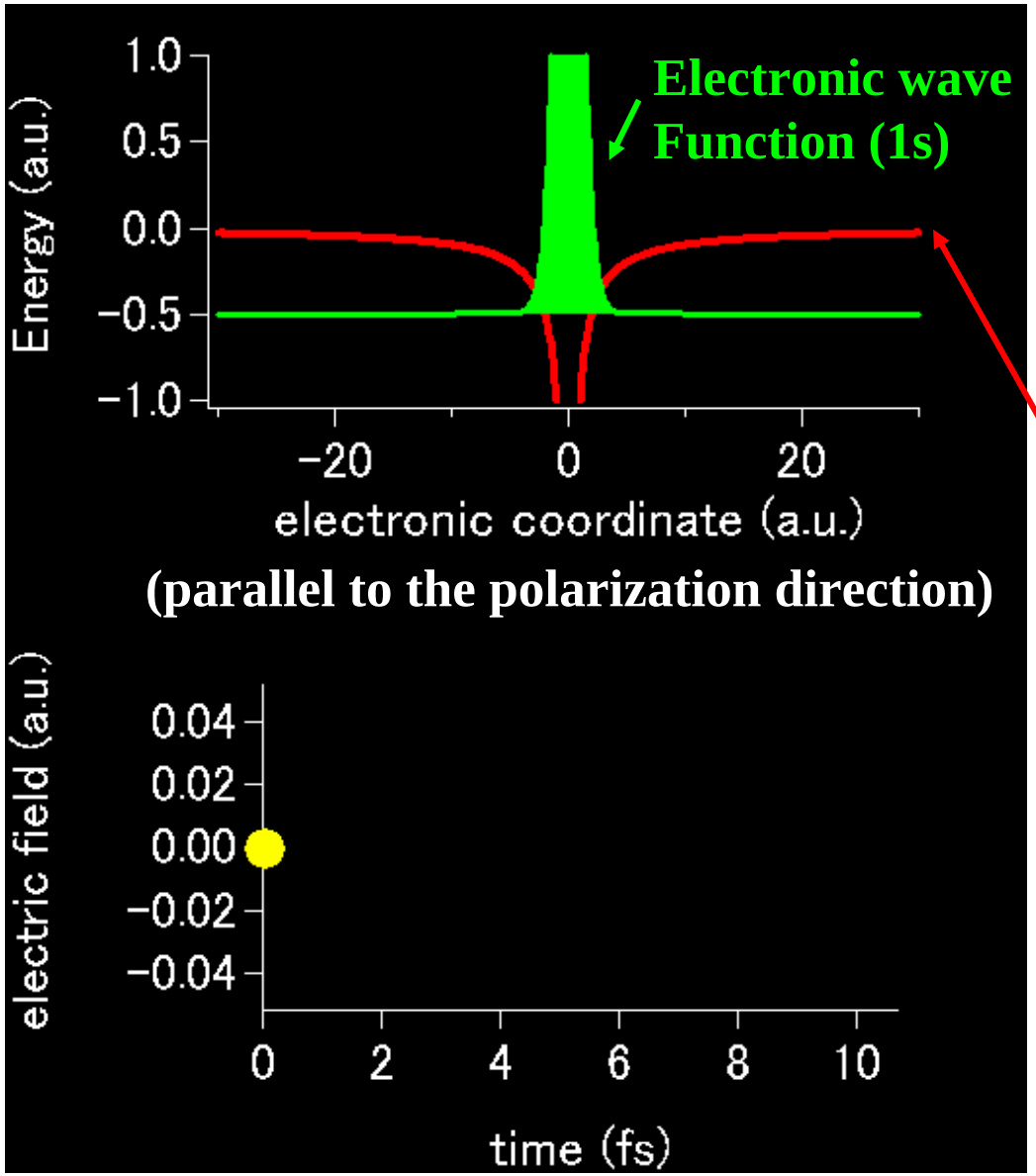

λ=760 nm

$I_{peak}=8.4\times10^{13}\mathrm{W/cm^2}$

(Keldysh parameter γ=1.2)

Coulomb+ dipole interaction

Ponderomotive radius of a rescattering electron

$$\propto \frac{ef_0}{m_e\omega^2} \quad \sim 100 \text{ Bohrs}$$

$\omega \rightarrow \omega/2$

3D grid points $\rightarrow$ 64 times

Sequential vs. nonsequential double ionization

Rescattering Model

P.B.Corkum, Phys. Rev.Lett. **71**,1994(1993).

Tunnel Ionization (ejection of one electron)

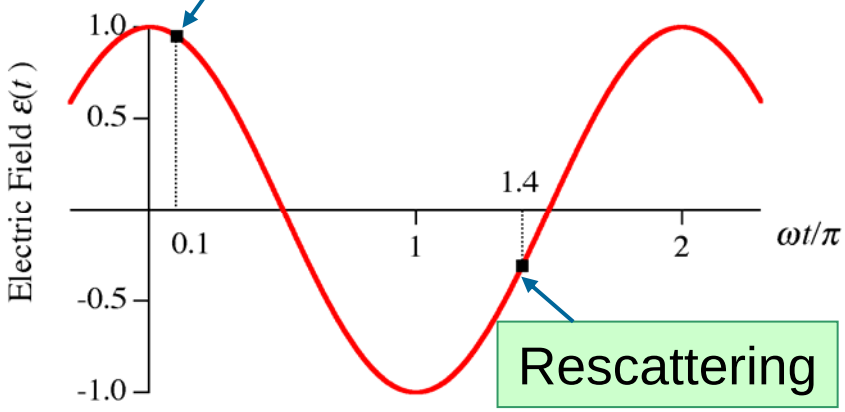

$t_i = 0.1\pi/\omega$

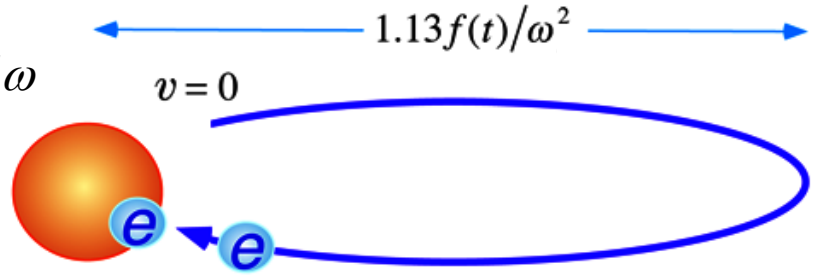

$t = 1.4\pi/\omega$

$v = 1.26 f(t)/\omega$ → Maximum rescattering energy: 3.17 U_p

Ponderomotive energy:

$$U_p = f^2(t)/4\omega^2$$

where $f(t)$ is the electric field amplitude.

Experimental Review

Th. Weber et al., Nature **405**, 658 (2000).

R.Dörner et al., Phys. Rep. **330**, 95 (2000).

λ= 800 nm

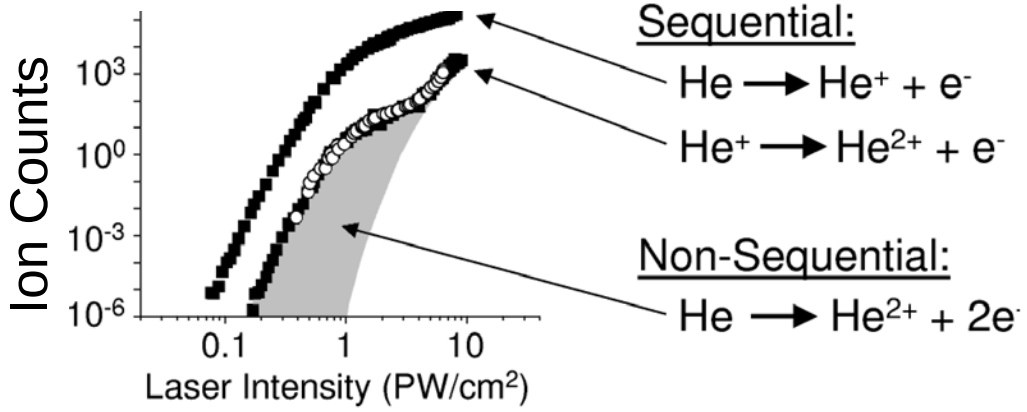

Intense-field many body S-matrix theory

A. Becker and F.H.M.Faisal, Phys.Rev. Lett. **84**, 3546 (2000).

Wave packet approach

K.T.Taylor et al. Laser Phys. **9**, 98(1999).

Tomographic imaging of molecular orbitals

Nature **432**, 867(2004)

J. Itatani[1,2], J. Levesque[1,3], D. Zeidler[1], Hiromichi Niikura[1,4], H. Pépin[3], J. C. Kieffer[3], P. B. Corkum[1] & D. M. Villeneuve[1]

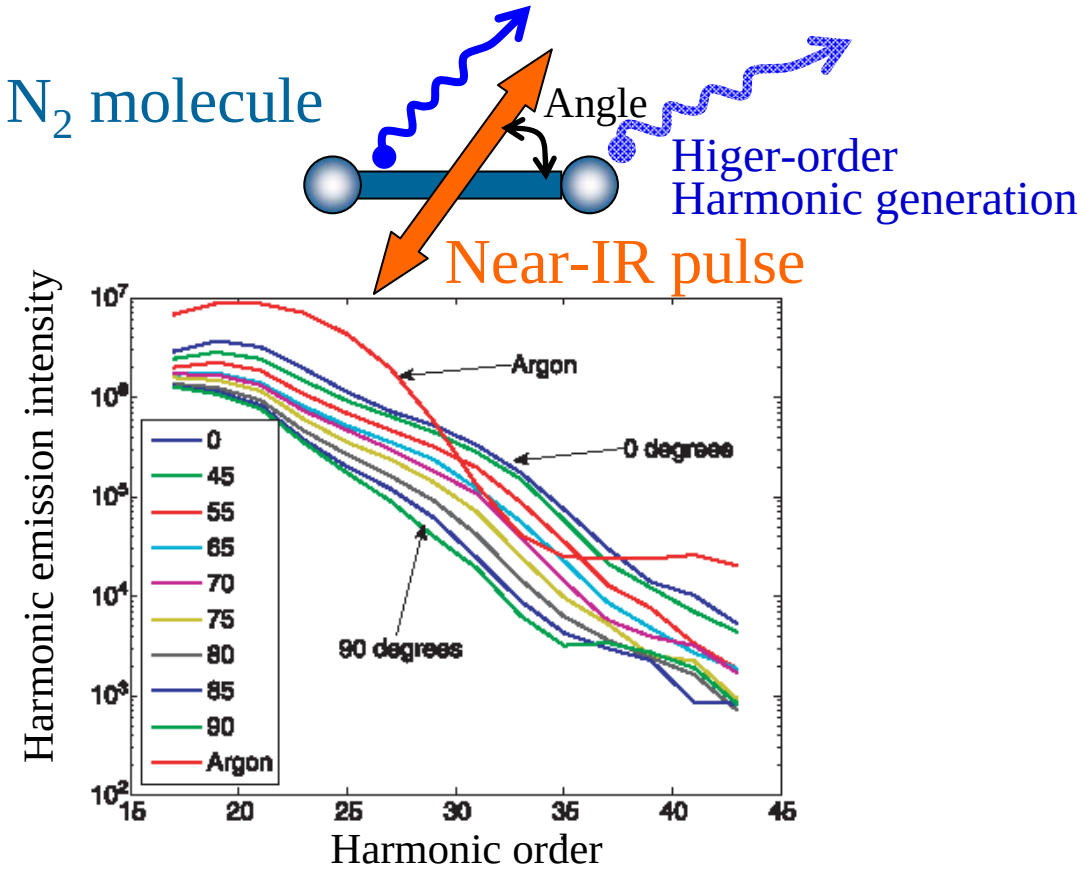

Figure 3 High harmonic spectra were recorded for N_2 molecules aligned at 19 different angles between 0 and 90° relative to the polarization axis of the laser. For clarity, only some of the angles have been plotted above. The high harmonic spectrum from argon is also shown; argon is used as the reference atom. Clearly the spectra depend on both the alignment angle and shape of the molecular orbital.

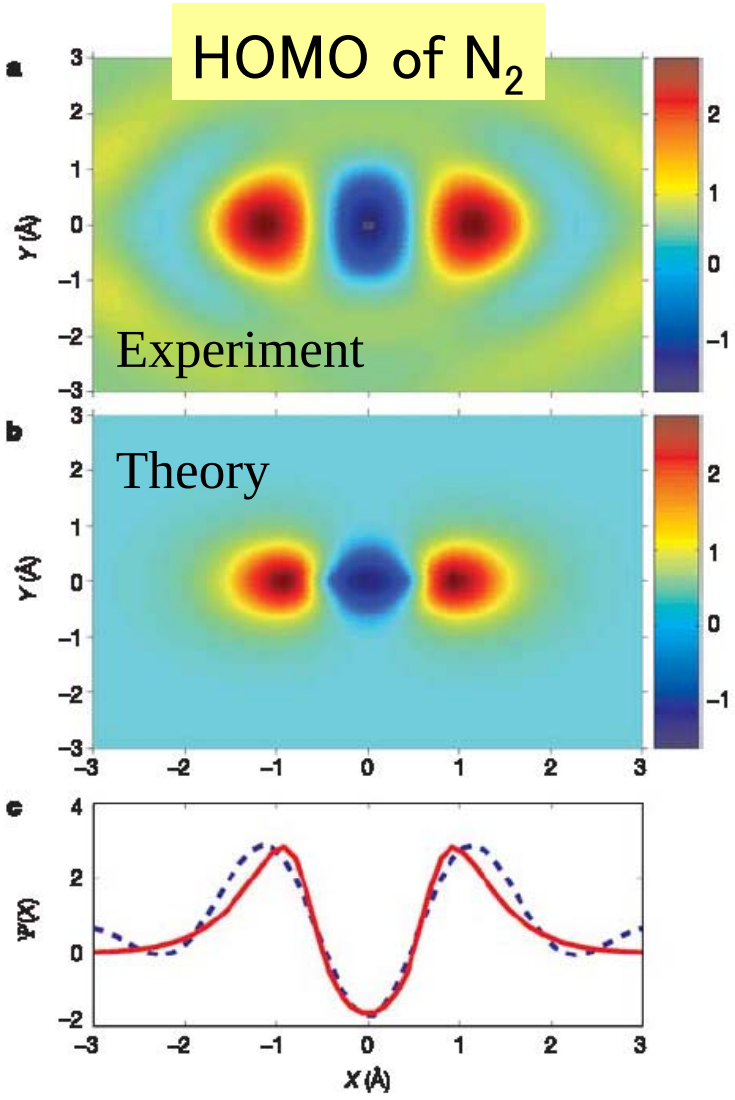

Figure 4 Molecular orbital wavefunction of N_2. **a**, Reconstructed wavefunction of the HOMO of N_2. The reconstruction is from a tomographic inversion of the high harmonic spectra taken at 19 projection angles. Both positive and negative values are present, so this is a wavefunction, not the square of the wavefunction, up to an arbitrary phase. **b**, The shape of the N_2 $2p\sigma_g$ orbital from an *ab initio* calculation. The colour scales are the same for both images. **c**, Cuts along the internuclear axis for the reconstructed (dashed) and *ab initio* (solid) wavefunctions.

Electron Dynamics: How to identify multielectron dynamics in ionization by intense near-IR laser pulses

Single active electron ionization

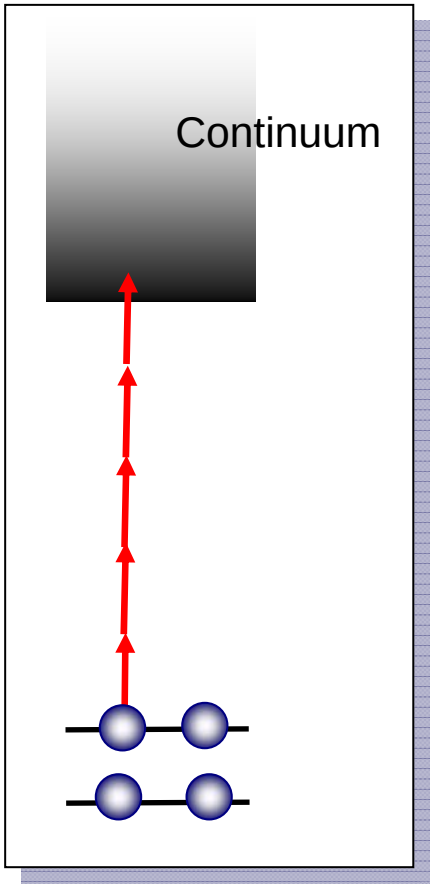

Linear > Circular

Ionization due to multielectron dynamics

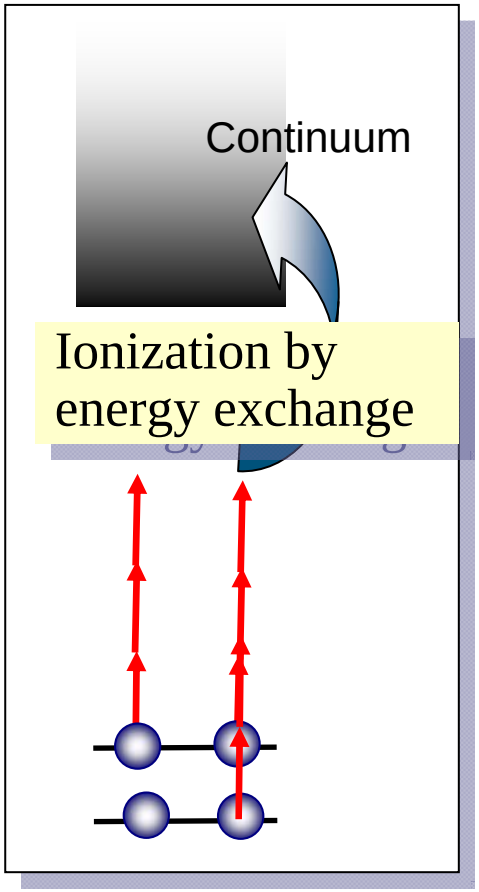

Linear = Circular

Experiment*:

Distinction in C_{60} ionization by linearly and circularly polarized pulses

If multielectron dynamics, no difference:
Only total pulse energy matters

*I.V. Hertel et al., PRL **102**, 023003 (2009) .

Multielectron dynamics of C60 above the doorway state

I. V. Hertel *et al*. Adv. At. Mol. Opt. Phys. 50, 219 (2005).

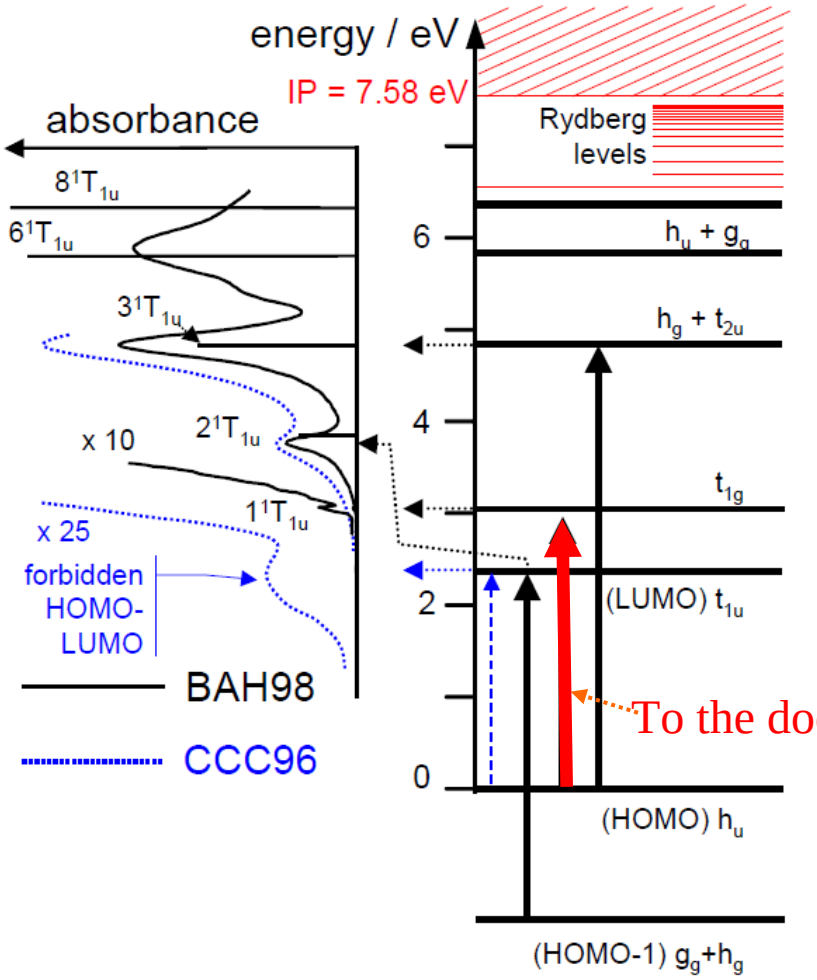

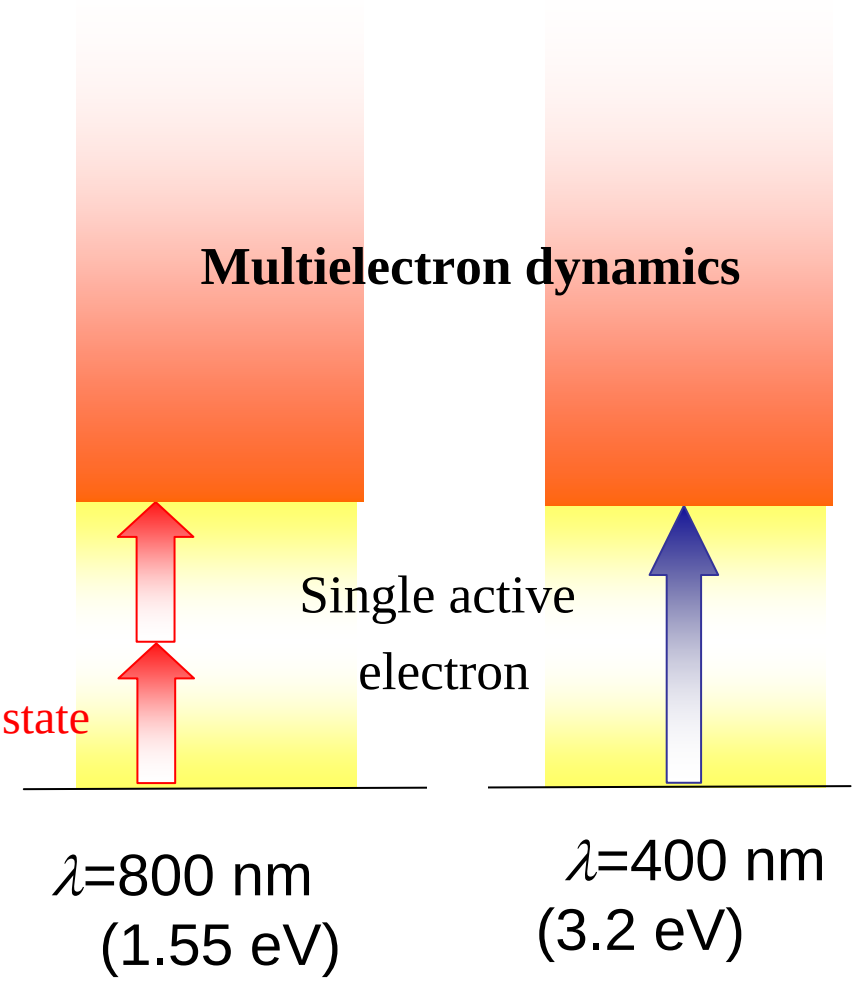

Multi-configuration time-dependent Hartree-Fock method (MCTDHF) – Beyond the mean field picture –

T. Kato and H. Kono, Chem. Phys. Lett. **392**, 533 (2004);J. Chem. Phys. **128**, 184102 (2008) .

MC Time-dependent many-body wave function: a unified way to treat different dynamical processes

$$\Phi(\vec{x}_1, \vec{x}_2, \cdots, \vec{x}_N; t) = \sum_I C_I(t) \quad \left\| \phi_{k_1}(\vec{x}_1)\phi_{k_2}(\vec{x}_2)\cdots\phi_{k_N}(\vec{x}_N) \right\|$$

Slater determinants with TD MOs

- Ionization dynamics of molecules in intense laser fields

Explicit inclusion of continuum states ⇨ grid point representation for MOs

Dirac-Frenkel variational principle

$$\langle \delta\,\Phi(t)| \left(i\hbar\partial_t - \hat{H}(t) \right) |\,\Phi(t)\rangle = 0$$

⇨ **H_2 & N_2**

(1) Equations of motion for CI coefficients $C_I(t)$

(2) Equations of motion for MOs (grid representation)

Other MCTD approaches

- J. Zanghellini, M. Kitzler, T. Brabec, and A. Scrinzi, J. Phys. B **37**, 763 (2004).
- Non-variational approach: T.T. Nguyen-Dang et al., J. Chem. Phys. **127,** 174107(2007).

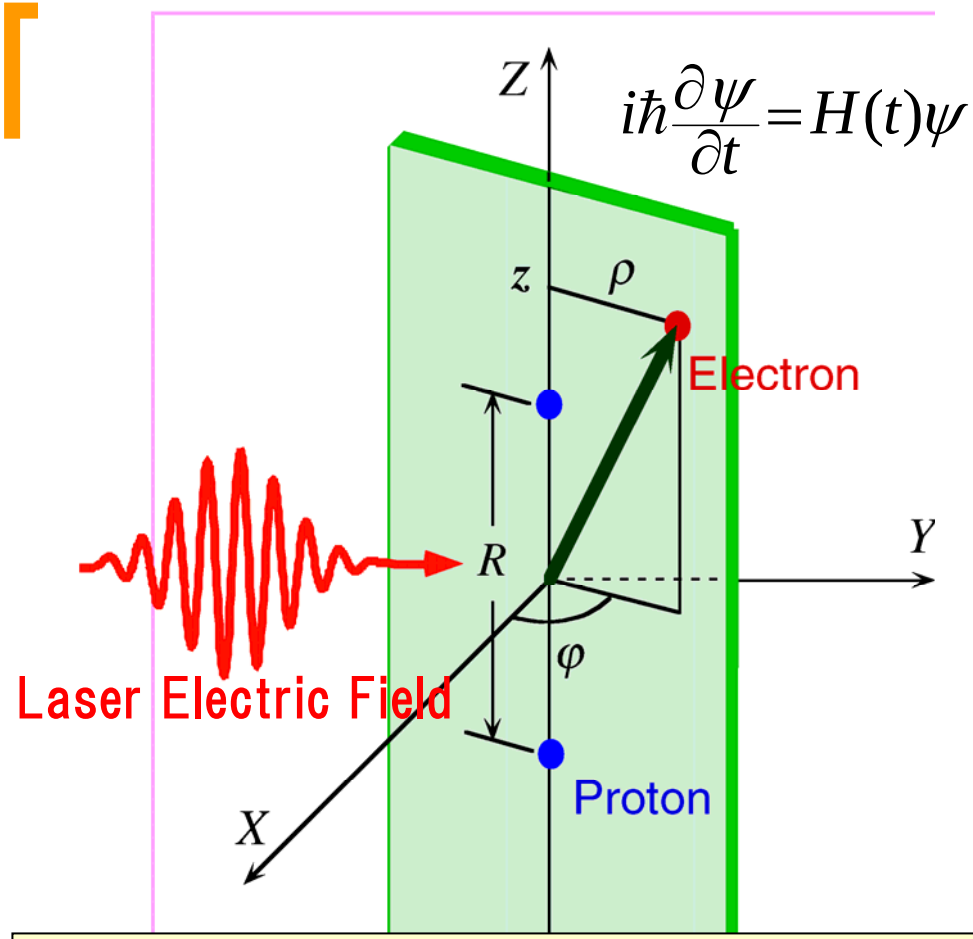

Transformation to remove cusps

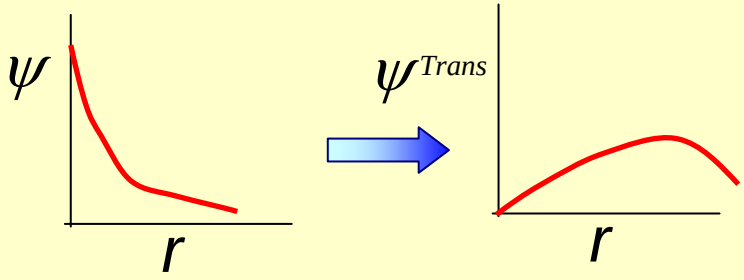

Electronic Wave function

DUAL TRANSFORMATION

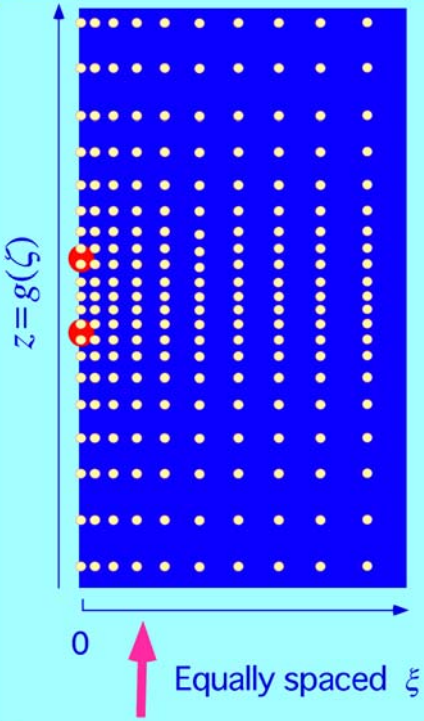

Variable Transformation

(i) Adjustable grid points

Large grid $\propto \frac{ef_0}{m_e\omega^2}$

$\rho=f(\xi)=\xi\left(\frac{\xi^n}{\xi^n+\alpha^n}\right)^\nu$

Hermitian Representation of the Discretized Hamiltonian

Normalization condition: $\int_0^\infty dR\int_0^\infty d\xi\int_{-\infty}^\infty d\zeta\left|\psi(\xi,\zeta,R)\right|^2=1$

Transformed wave function:

$\psi(\xi,\zeta,t)=\sqrt{f(\xi)f'(\xi)g'(\zeta)}\times$ (original wave function)

(ii) Transformed wavefunction=0 at ρ=0

(iii) Finite difference ≈Differential

(iv) Transformation of the Hamiltonian

I. Kawata & H. Kono, J. Chem. Phys. **111**, 9498 (1999).

Application to H_2

(R=1.6 a_0, 9 MOs)

I_{peak}=5.8 × 10^{13} W/cm^2

λ=760 nm

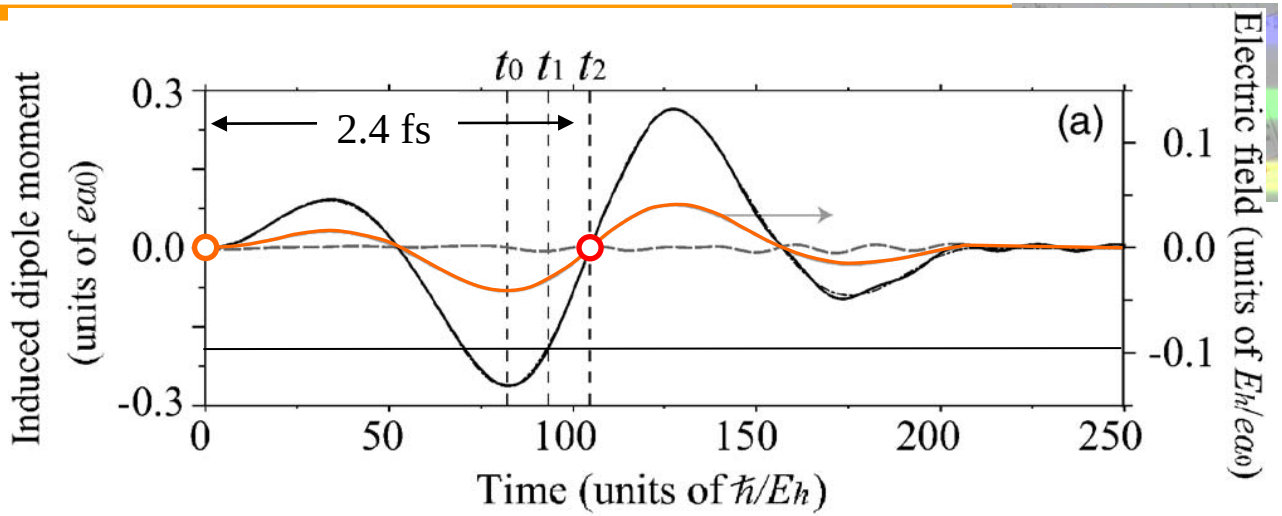

Cylindrical coordinates for H_2

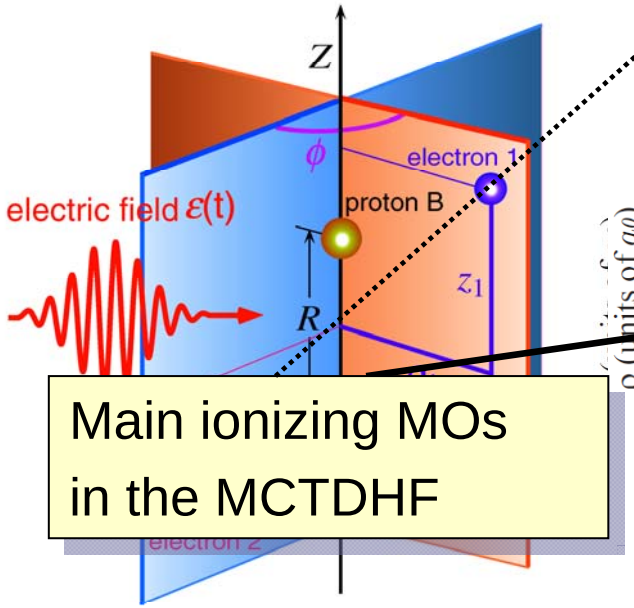

Main ionizing MOs in the MCTDHF

Electron densities of natural orbitals (Log scale)

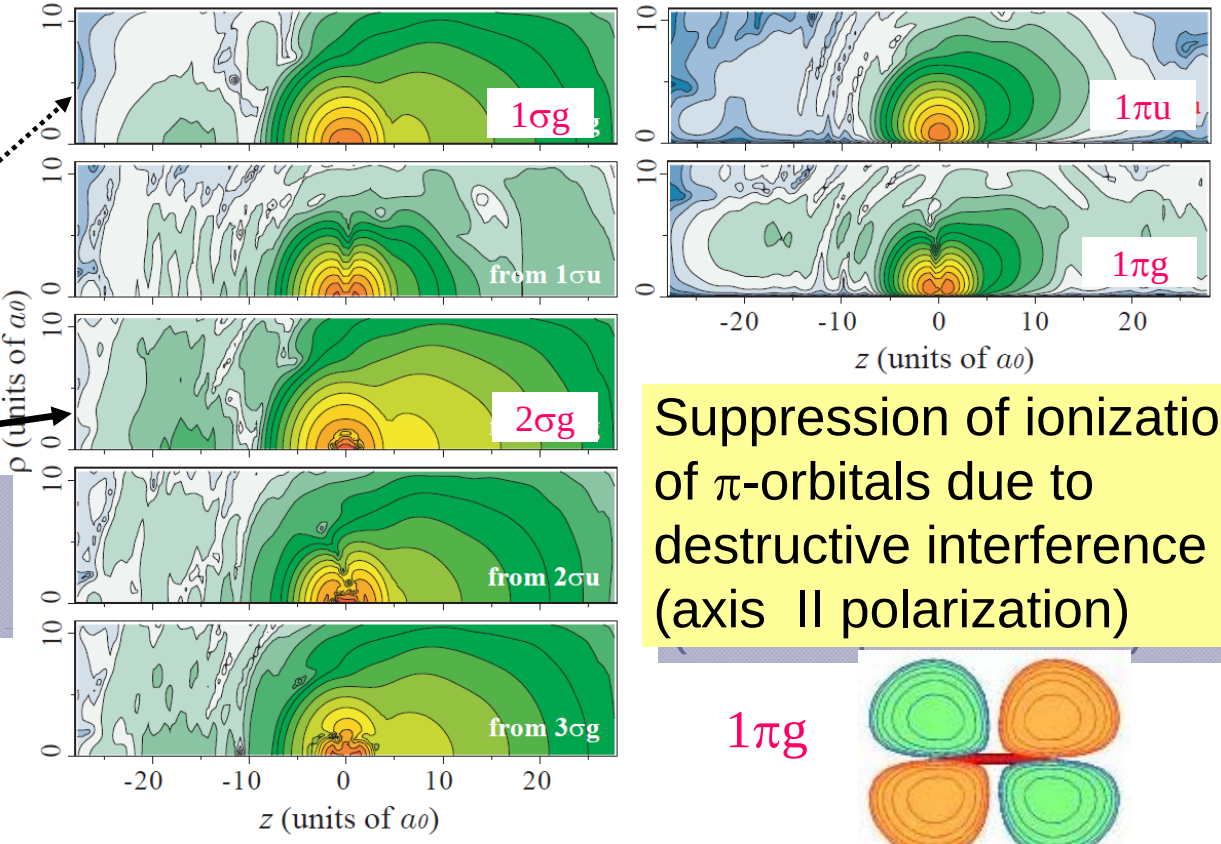

Suppression of ionization of π-orbitals due to destructive interference (axis ∥ polarization)

1πg

Ionization from individual natural orbitals

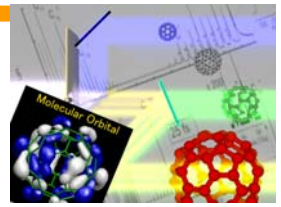

Change in the occupation number $\rho(\boldsymbol{r},\boldsymbol{r}',t)=\sum_{j}^{N_O} w_j(t)\phi_j^*(\boldsymbol{r}',t)\phi_j(\boldsymbol{r},t),$

$$\Delta w_j(t) = \Delta w_j^{\text{absorb}} + \Delta w_j^{\text{exchange}}$$

absorbed at the boundaries population exchange

⇩

Ionization

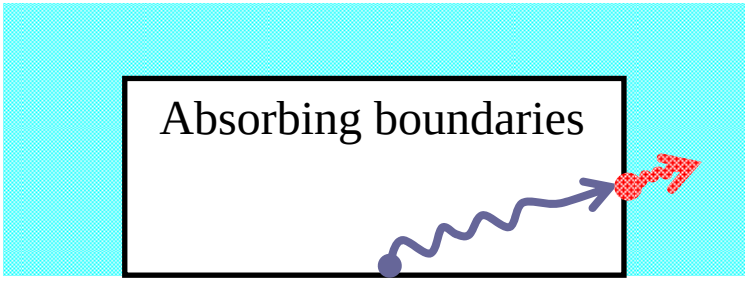

MC wave function at time t after one-step of time propagation

⇩

Reduction in the MO norm at the absorbing boundary

⇩

Renormalization of MO norms

⇩

Recalculation of CI coefficients

① $\Phi^{(a)} = \sum_I C_I^{(a)} \Phi_I^{(a)}$ for TDMO $\{\varphi_j^{(a)}\}$ → $w_j^{(a)}$

② $\Phi^{(b)} = \sum_I C_I^{(a)} \Phi_I^{(b)}$ for absorbed $\{\varphi_j^{(b)}\}$

③ $\Phi^{(c)} = \sum_I C_I^{(c)} \Phi_I^{(c)}$ for ortho-normalized $\{\varphi_j^{(c)}\}$ → $w_j^{(c)}$

$$\Delta w_j^{\text{absorb}} = w_j^{(a)} - w_j^{(c)}$$

H_2分子 ($R = 1.6a_0$) の自然軌道からのイオン化率およびイオン化の様子 (時刻 $t = 1.5T_c$)

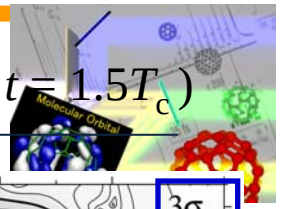

λ = 760 nm, $I_{peak} = 5.8 \times 10^{13}$ W/cm²

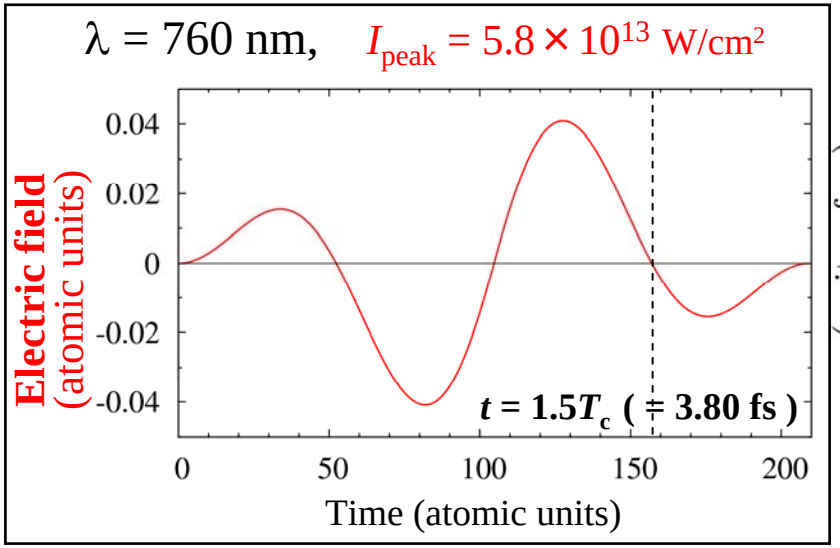

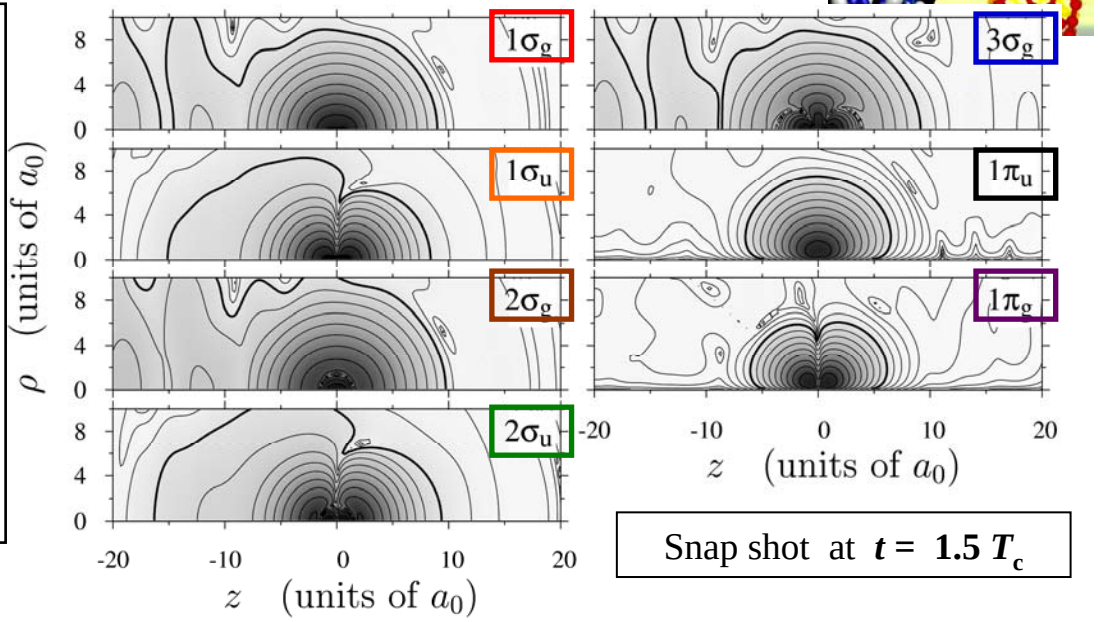

Snap shot at $t = 1.5\ T_c$

Accumulated reduction through MOs

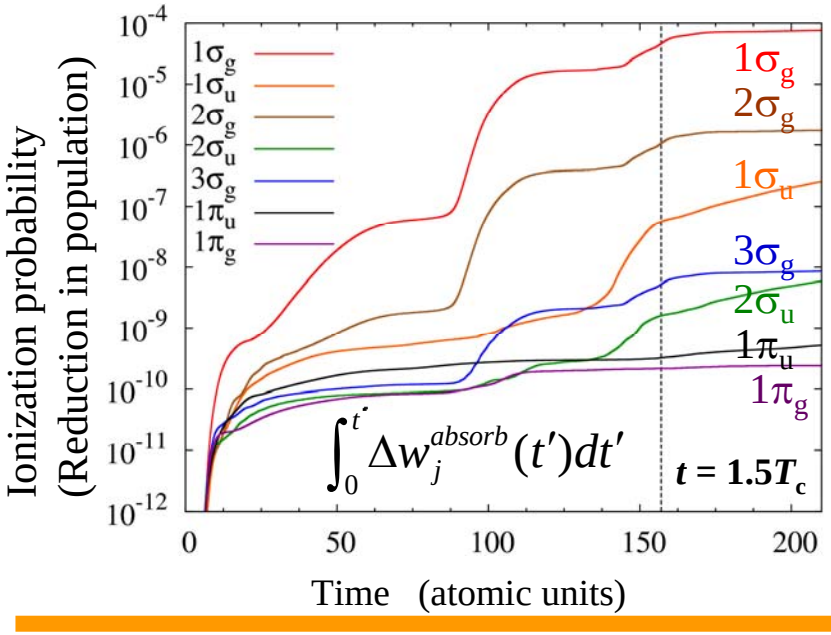

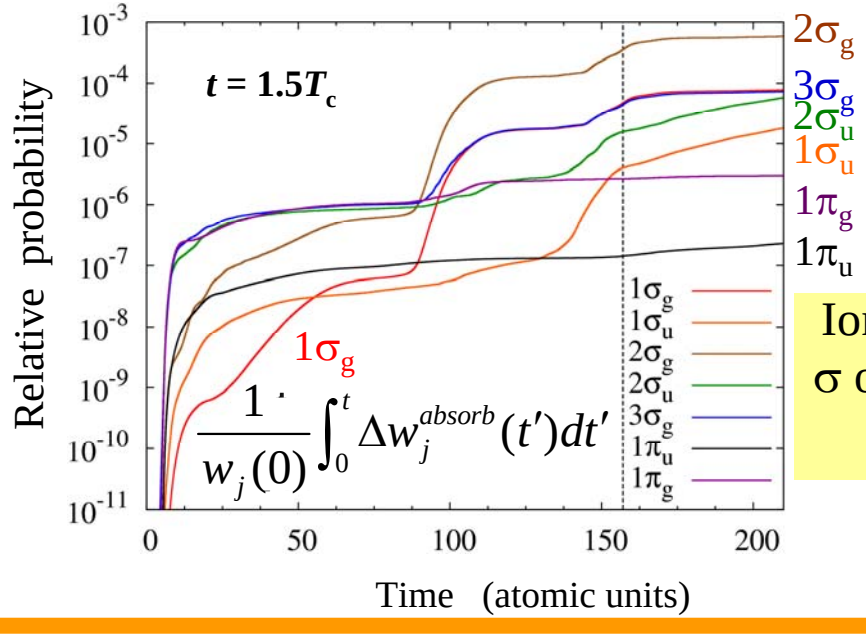

Ionization
σ orbitals:
g>u

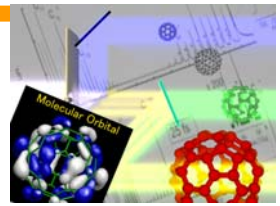

Road to “time-dependent” chemical potential

T. Kato & H. Kono, Chem. Phys. **366**, 46 (2009), special issue on “Attosecond chemistry” eds. Andre D. Bandrauk, Jörn Manz, and Mark Vrakking

Chemical potential $\mu_j(t)$ of a two-electron system

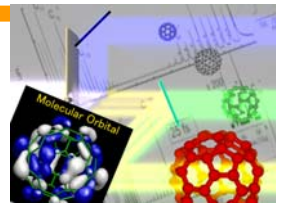

One-to-one correspondence for natural orbitals:

Occupation number $w_j = |C_j|^2$

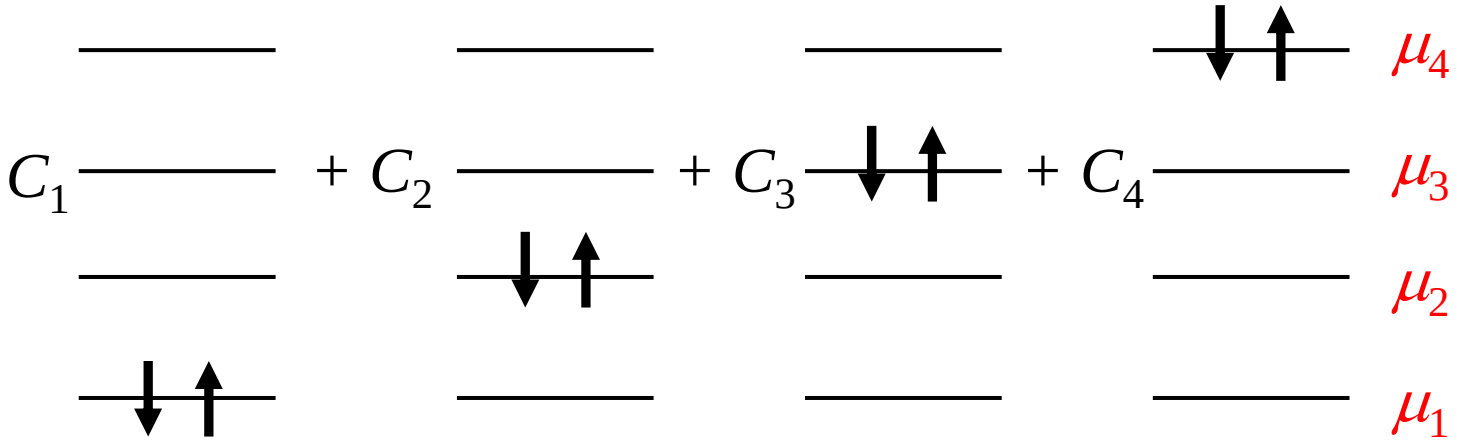

Chemical potential

Chemical potential for natural orbital *j*

$$\mu_j = h_{jj} + \frac{1}{2}\left[j_\beta j_\beta \middle| j_\alpha j_\alpha \right] + \frac{1}{2}\mathrm{Re}\left[\sum_{k \neq j}^{N_O} \left[k_\beta j_\beta \middle| k_\alpha j_\alpha \right] \frac{C_k}{C_j^*} \right]$$

One-electron — Coulomb — **Correlation**

where

$$[ki|lj] = \frac{1}{4\pi\epsilon_0} \int d\vec{x}_1\, d\vec{x}_2\, \phi_k^*(\vec{x}_1)\phi_i(\vec{x}_1) \frac{e^2}{|\vec{r}_1 - \vec{r}_2|} \phi_l^*(\vec{x}_2)\phi_j(\vec{x}_2)$$

$$\Longrightarrow \quad E(t) = \sum_j^{N_O} w_j(t)\, \mu_j(t)$$

Chemical potential change of H_2 & HeH^+ in a near-IR field (R=1.6 a_0)

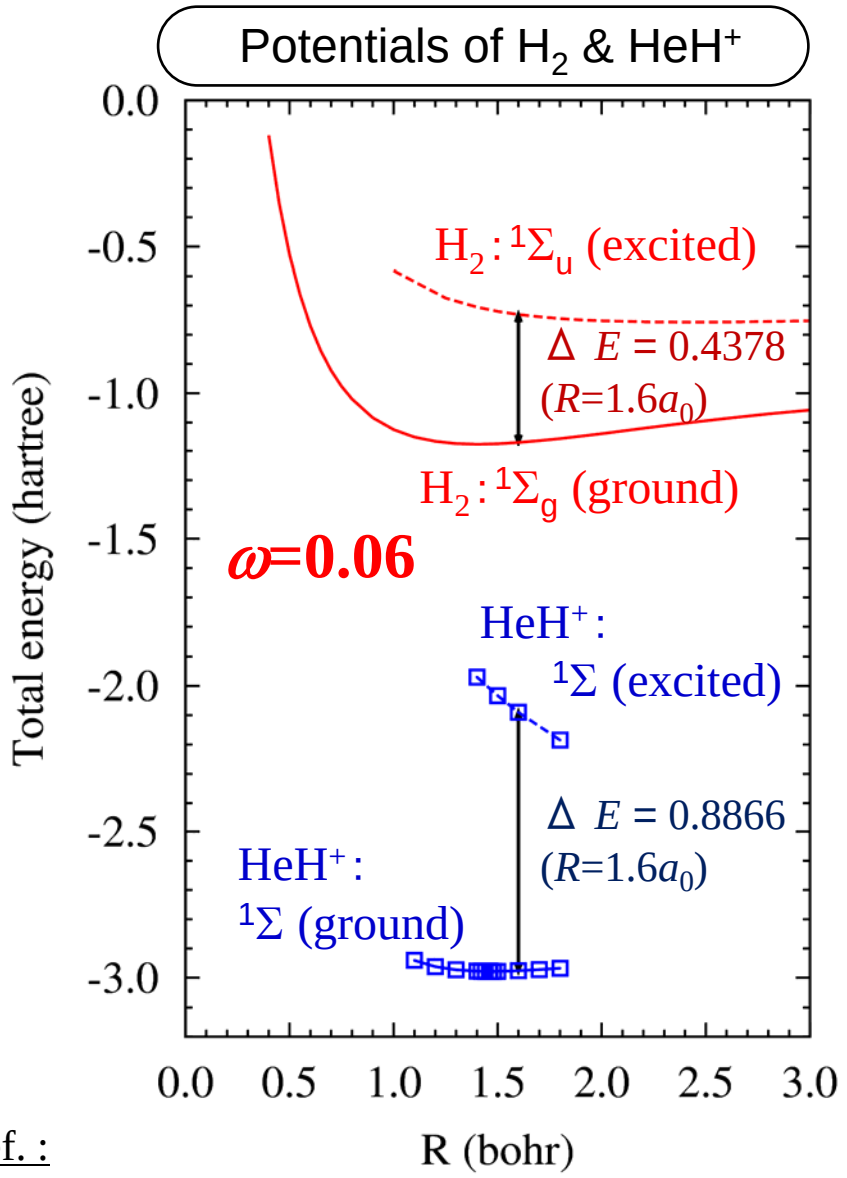

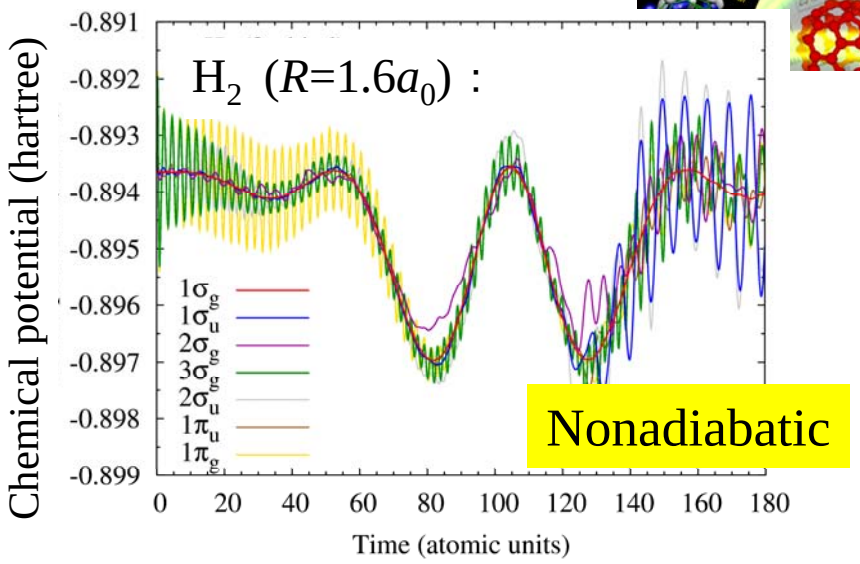

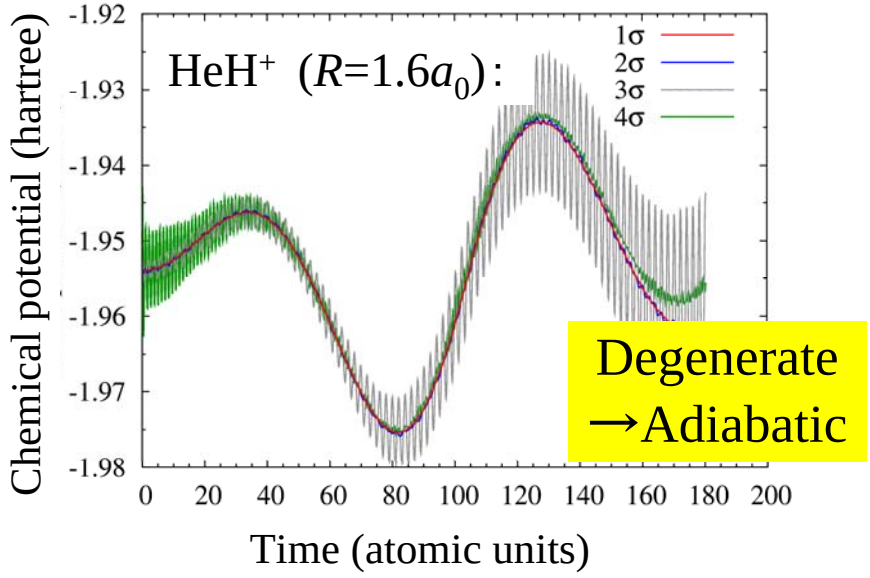

Ref. :

H_2 : W.Kolos and L.Wolniewicz, J. Chem. Phys. **43**, 2429 (1965).

HeH^+ : L.Wolniewicz, J. Chem. Phys. **43**, 1087 (1965).

Light-intensity : $I_{peak} = 1.0 \times 10^{14}$ W/cm^2

Wavelength : λ = 760 nm (T_c = 2.53 fs)

Energy supply through the interaction with the field

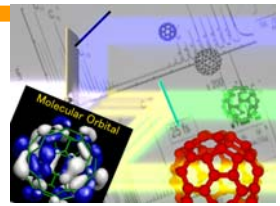

- The total energy supplied to the system from the field $\boldsymbol{\mathcal{E}}(t)$ per unit time within the dipole approximation in the length gauge:

$$\frac{d}{dt}E(t)=\frac{d}{dt}\langle\Phi(t)|\hat{H}(t)|\Phi(t)\rangle=\langle\Phi(t)|e\sum_j \boldsymbol{r}_j|\Phi(t)\rangle\cdot\frac{d}{dt}\boldsymbol{\mathcal{E}}(t)=-\boldsymbol{d}(t)\cdot\frac{d}{dt}\boldsymbol{\mathcal{E}}(t)$$

where the total electronic Hamiltonian is given by $\hat{H}(t)=\hat{H}_0+e\sum_j \boldsymbol{r}_j\cdot\boldsymbol{\mathcal{E}}(t)$

- Energy gain of the system from the field

$$E(t)-E(0)=-\int_0^t \boldsymbol{d}(t')\cdot\frac{d}{dt'}\boldsymbol{\mathcal{E}}(t')dt'=-\boldsymbol{d}(t)\cdot\boldsymbol{\mathcal{E}}(t)+\int_0^t\frac{d[\boldsymbol{d}(t')]}{dt'}\cdot\boldsymbol{\mathcal{E}}(t')dt'$$

$$\langle\Phi(t)|\hat{H}_0|\Phi(t)\rangle-\langle\Phi(0)|\hat{H}_0|\Phi(0)\rangle=\int_0^t\frac{d[\boldsymbol{d}(t')]}{dt'}\cdot\boldsymbol{\mathcal{E}}(t')\,dt'\geq 0$$

T. Kato & H. Kono, Chem. Phys. **366**, 46 (2009), special issue on “Attosecond chemistry” eds. Andre D. Bandrauk, Jörn Manz, and Mark Vrakking

$$E(t)-E(0)-\underbrace{\left[-\boldsymbol{d}(t)\cdot\boldsymbol{\mathcal{E}}(t)\right]}_{\text{Reference energy}}=\int_0^t \frac{d\left[\boldsymbol{d}(t')\right]}{dt'}\cdot\boldsymbol{\mathcal{E}}(t')\,dt'$$

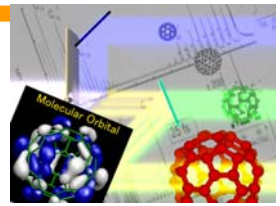

Introduction of natural orbitals

Diagonal representation of the one –electron density:

$$\rho(\boldsymbol{r},t)=\sum_j^{N_O} w_j(t)\phi_j^*(\boldsymbol{r},t)\phi_j(\boldsymbol{r},t),\qquad 0\le w_j(t)\le 1\qquad \sum_j^{N_O} w_j(t)=N_{\text{electron}}$$

where $\{\phi_j(\boldsymbol{r})\}$ are natural orbitals obtained from $\Phi(t)$ (unitary transformation of TD-MOs) and $\{w_j(t)\}$ are occupation numbers. N_o is the number of spin orbitals.

Advantage of natural orbitals:

- uniquely determined for the electron density (i.e., the electronic wave function)
- the energy of the one-body interaction $e\sum_j \boldsymbol{r}_j\cdot\boldsymbol{\mathcal{E}}(t)$ is given by the sum of the diagonal elements

$$E(t)-E(0)-\underbrace{\left[-\boldsymbol{d}(t)\cdot\boldsymbol{\mathcal{E}}(t)\right]}_{\text{Reference energy}}=\int_0^t \frac{d\left[\boldsymbol{d}(t')\right]}{dt'}\cdot\boldsymbol{\mathcal{E}}(t')\,dt'=\sum_{j=1}^{N_O}\int_0^t \frac{d\,w_j(t')\boldsymbol{d}_j(t')}{dt'}\cdot\boldsymbol{\mathcal{E}}(t')\,dt'$$

Energy injected into $\phi_j(t)$

where $\boldsymbol{d}_j(t)$ are the dipole moments of *natural orbitals* $\phi_j(t)$

$$\boldsymbol{d}_j(t)=-e\langle\phi_j(t)|\boldsymbol{r}|\phi_j(t)\rangle$$

How much energy do the individual MOs gain from the field?
How much energy is then exchanged among MOs?

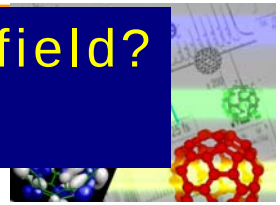

$$E(t) - E(0) - \left[-\boldsymbol{d}(t)\cdot\boldsymbol{\mathcal{E}}(t)\right] = \sum_{j=1}^{N_O} \int_0^t \frac{d\, w_j(t')\boldsymbol{d}_j(t')}{dt'} \cdot \boldsymbol{\mathcal{E}}(t')\, dt'$$

$$\Downarrow$$

$$\sum_{j=1}^{N_O} w_j(t) \underbrace{\left[\mu_j(t) - \mu_j(0) + \boldsymbol{d}_j(t)\cdot\boldsymbol{\mathcal{E}}(t)\right]}_{\Delta\bar{\varepsilon}_j(t)} \approx \sum_{j=1}^{N_O} w_j(t) \underbrace{\int_0^t \frac{d\left[\boldsymbol{d}_j(t')\right]}{dt'} \cdot \boldsymbol{\mathcal{E}}(t')\, dt'}_{S_j(t)}$$

(1) Injected energy: Energy supply from the field to the natural orbital j through the radiative dipole interaction: $S_j(t)$

(2) Quantification of energy exchange: Total energy decomposition into "chemical potentials": $\Delta\bar{\varepsilon}_j(t)$

Comparison between $S_j(t)$ and $\Delta\bar{\varepsilon}_j(t)$

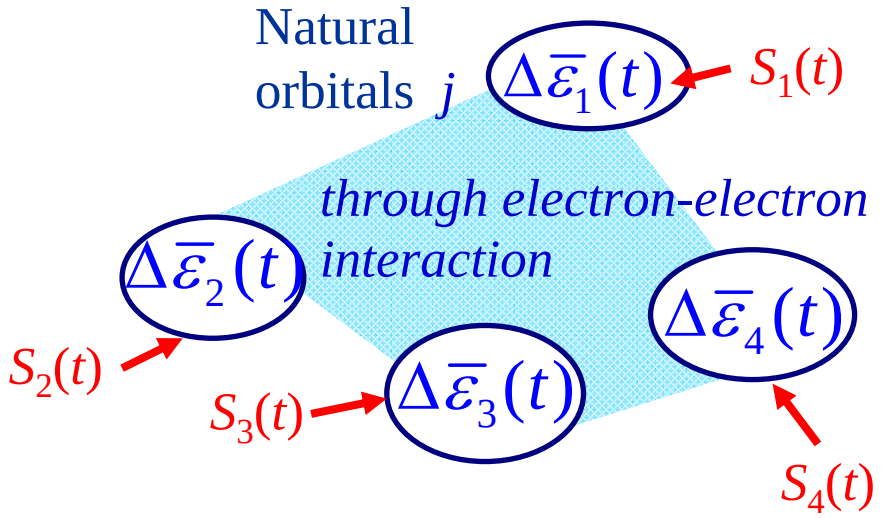

Orbital population

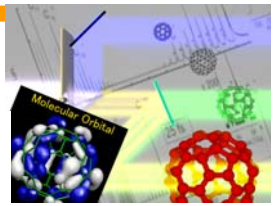

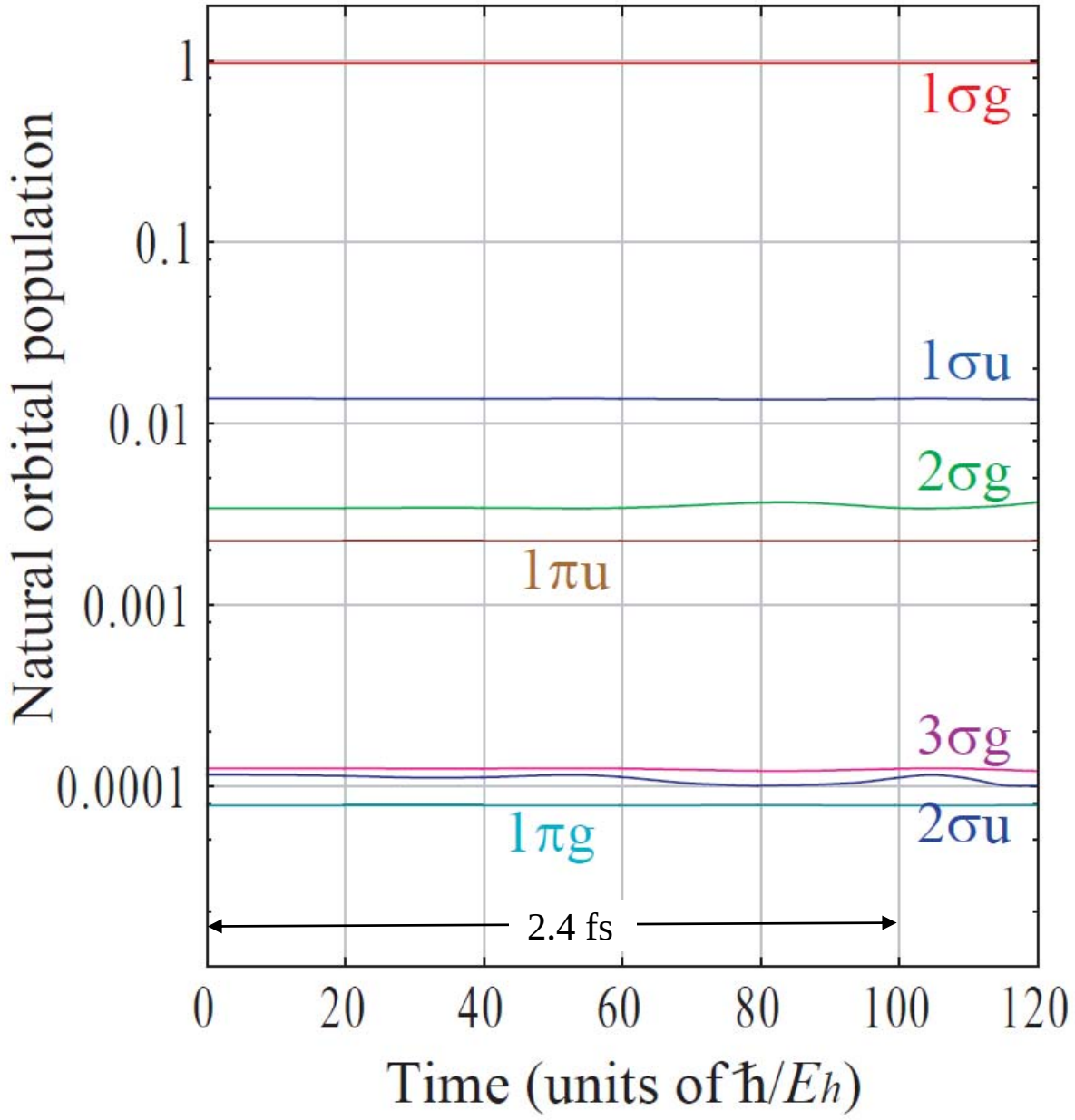

Chemical potential change $\Delta\bar{\epsilon}_j(t)$ and $S_j(t)$

Energy supplied from the field to the natural orbital $\phi_j(t)$:

$$S_j(t) = \int_0^t \frac{d\left[\boldsymbol{d}_j(t')\right]}{dt'} \cdot \boldsymbol{\varepsilon}(t')dt'$$

$\Delta\bar{\epsilon}_j(t) \approx S_j(t)$

Spectator orbital

$\Delta\bar{\epsilon}_j(t) > S_j(t)$

Energy accepting orbital

$2\sigma_g$ is an energy accepting orbital
→ efficient ionizing MO

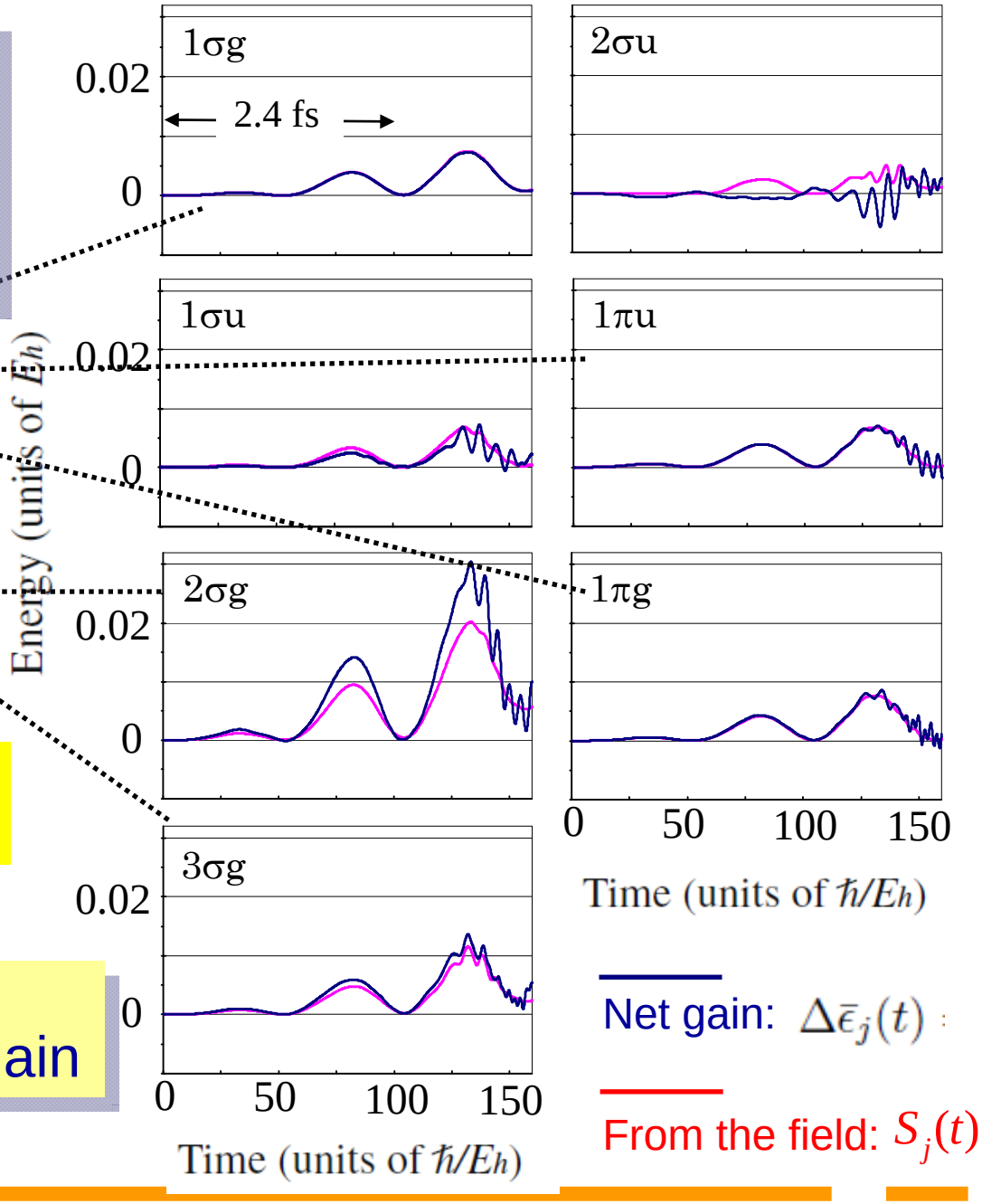

Net gain: $\Delta\bar{\epsilon}_j(t)$

From the field: $S_j(t)$

Quantification of energy exchange in the sub-fs domain

Decomposition of the chemical potential

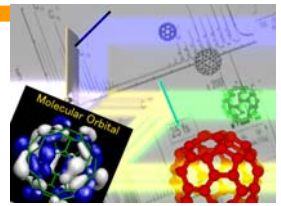

$$\Delta\overline{\varepsilon}_j(t) = \mu_j(t) - \mu_j(0) + \boldsymbol{d}_j(t)\cdot\boldsymbol{\mathcal{E}}(t)$$

$$= \left\{h_{jj}(t) - h_{jj}(t{=}0) \;\; + \boldsymbol{d}_j(t)\cdot\boldsymbol{\mathcal{E}}(t)\right\}$$

one-electron

$$+\frac{1}{2}\left\{\left[j_\beta j_\beta \middle| j_\alpha j_\alpha\right](t) - \left[j_\beta j_\beta \middle| j_\alpha j_\alpha\right](t{=}0)\right.$$

two-electron

$$\left. + \mathrm{Re}\left[\sum_{k\neq j}^{N_O}\left[k_\beta j_\beta \middle| k_\alpha j_\alpha\right]\frac{C_k}{C_j^*}(t) - \left[k_\beta j_\beta \middle| k_\alpha j_\alpha\right]\frac{C_k}{C_j^*}(t=0)\right]\right\}$$

Correlation

Correlation Energy Change for $1\sigma_g$

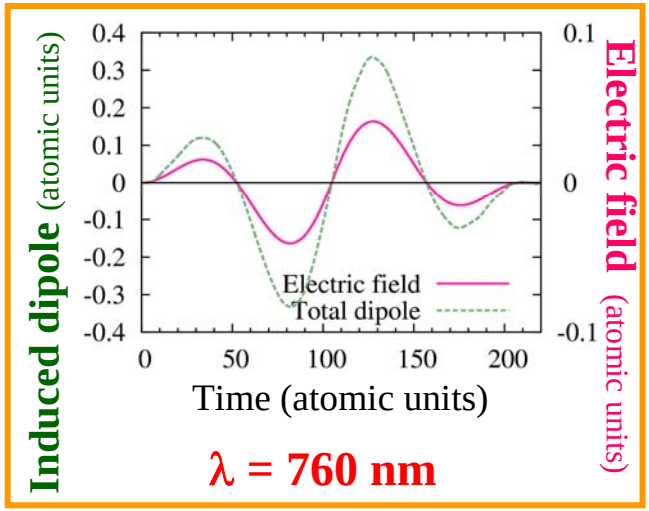

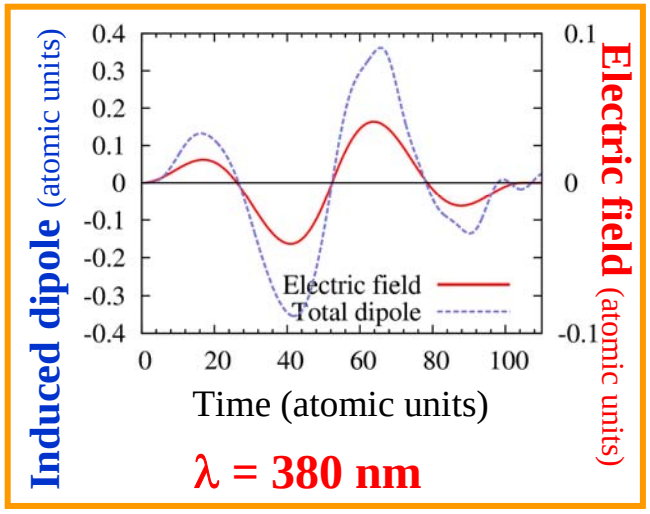

$$\Delta\bar{\varepsilon}(t)_{1\sigma_g} \approx S_{1\sigma_g}(t)$$

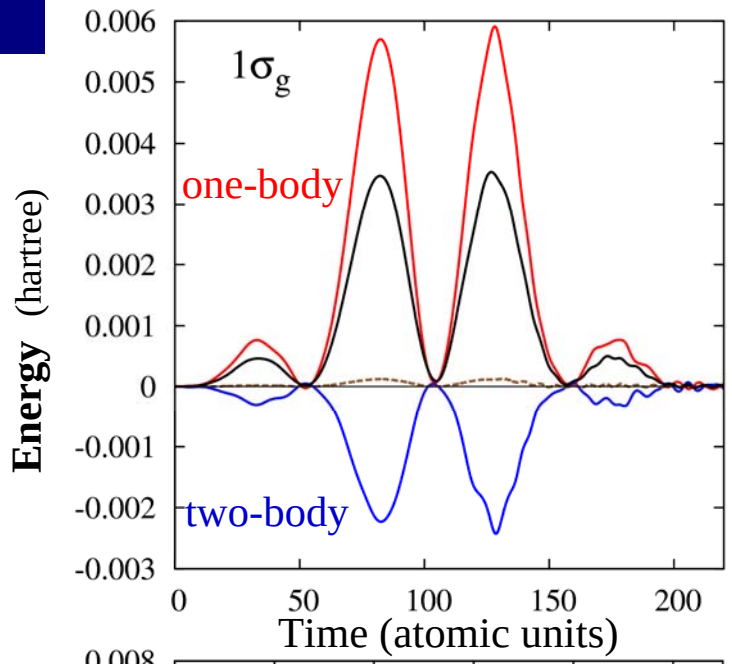

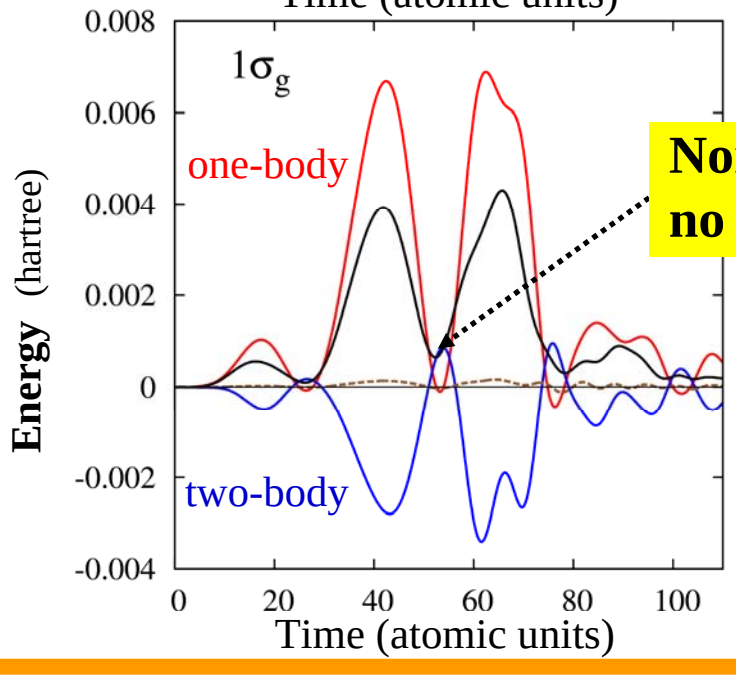

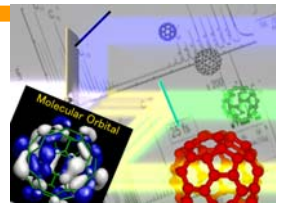

$\Delta\bar{\varepsilon}(t)_{1\sigma_g}$: ——

Correlation energy Change: ·····

Nonadiabatic but no energy exchange

Correlation Energy Change for $2\sigma_g$

$\Delta\bar{\varepsilon}(t)_{2\sigma_g}$: —— Correlation energy Change: ·····

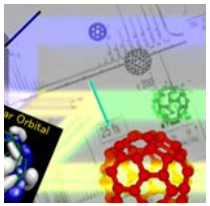

$\Delta\bar{\varepsilon}(t)_{2\sigma_g} > S_{2\sigma_g}(t)$

λ = 760 nm

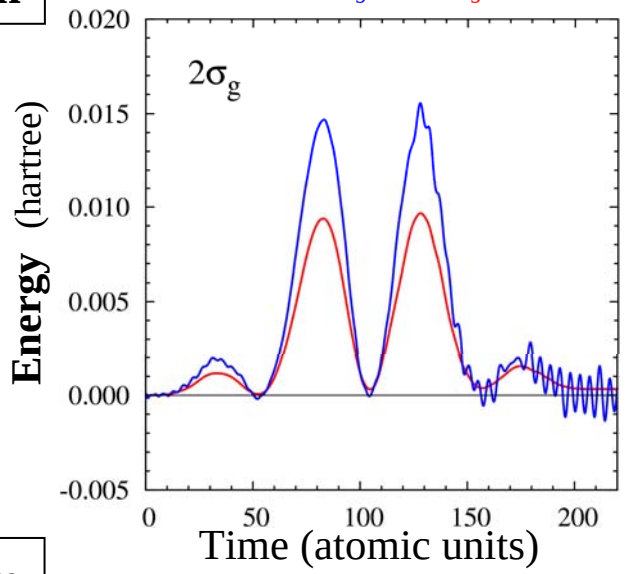

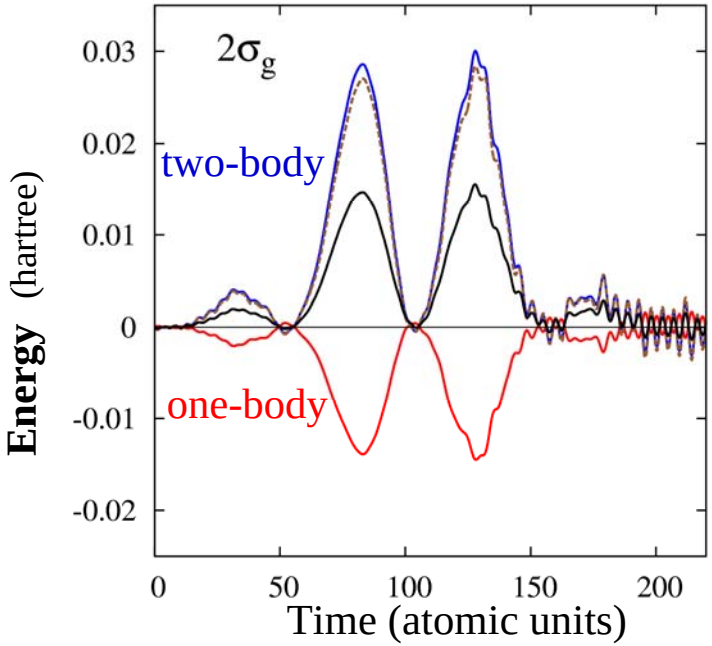

λ = 380 nm

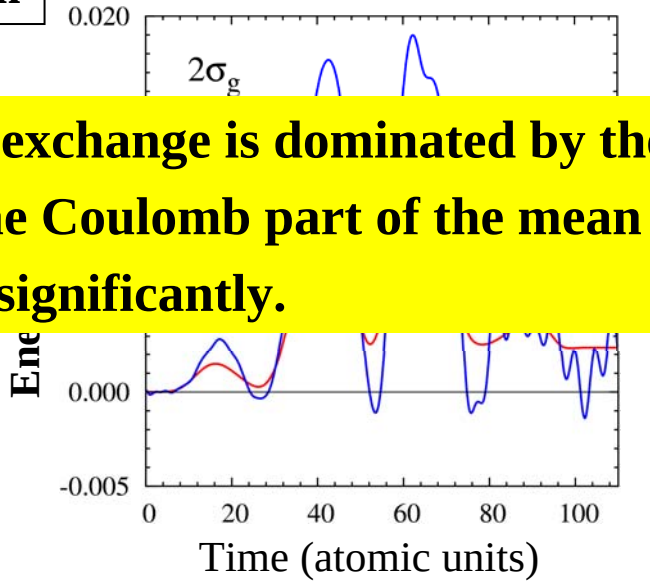

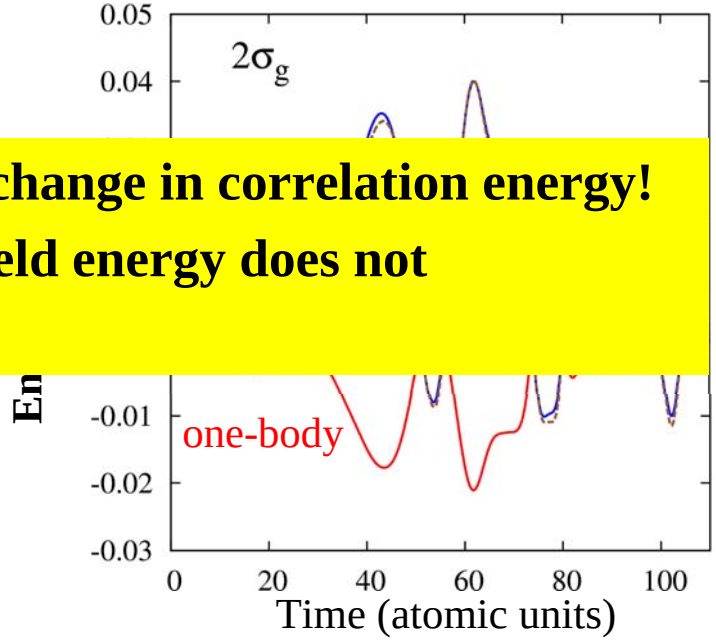

Energy exchange is dominated by the change in correlation energy! while the Coulomb part of the mean field energy does not change significantly.

Ionization dynamics in H_2 at R=1.6 a_0 (MCTDHF by T. Kato)

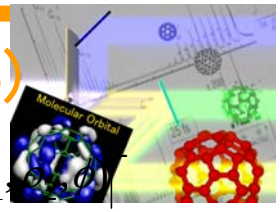

Reduced density map (*Log scale*)

$$\bar{P}(z_1,z_2)=\int d\rho_1\int d\rho_2\int d\phi\rho_1\rho_2\left|\Psi(z_1,z_2,\rho_1,\rho_2,\phi)\right|$$

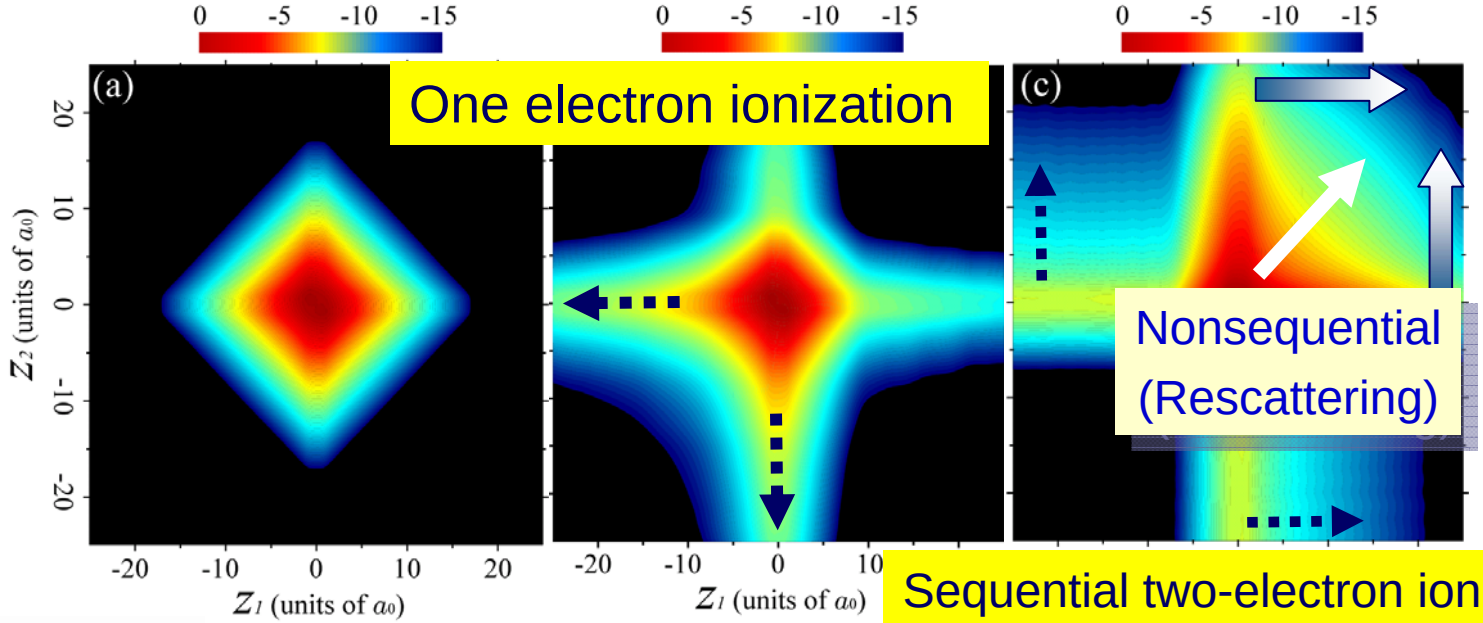

One electron ionization

Nonsequential (Rescattering)

Sequential two-electron ionization

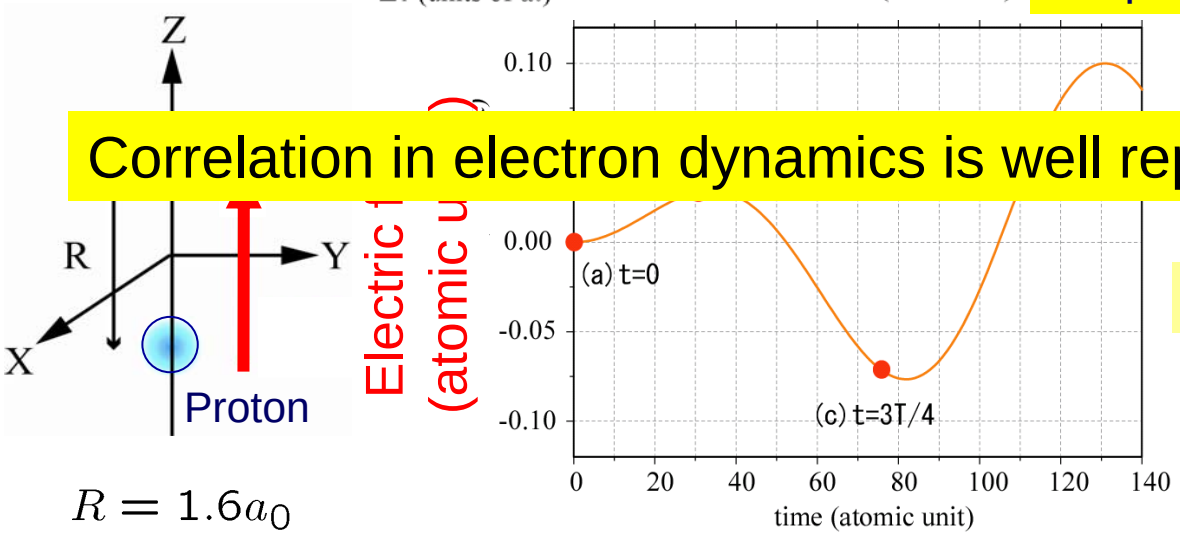

λ=760 nm

10^{14} W/cm^2

Correlation in electron dynamics is well reproduced

$R = 1.6a_0$

cf. Dual Transformation Method

K. Harumiya et al. J. Chem. Phys. **113**, 8953(2000) ; K. Harumiya, H. Kono, Y. Fujimura, I. Kawata, A.D. Bandrauk, Phys. Rev. A **66**, 043403 (2002).

Spatial distribution of the correlation energy: Correlation energy density

$$E_C = \frac{1}{2}\sum_{i}\sum_{j\neq i}\sum_{k\neq i\neq j}\sum_{\ell\neq k\neq i\neq j}\left\langle i(\boldsymbol{r}_1)k(\boldsymbol{r}_2)\left|\frac{1}{|\boldsymbol{r}_1-\boldsymbol{r}_2|}\right|j(\boldsymbol{r}_1)\ell(\boldsymbol{r}_2)\right\rangle\Gamma_{ij,k\ell}$$

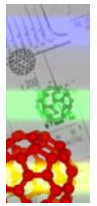

$$E_C(\boldsymbol{r}_1) = \frac{1}{2}\sum_{i}\sum_{j\neq i}\sum_{k\neq i\neq j}\sum_{\ell\neq k\neq i\neq j}\int i(\boldsymbol{r}_1)k(\boldsymbol{r}_2)\frac{1}{|\boldsymbol{r}_1-\boldsymbol{r}_2|}j(\boldsymbol{r}_1)\ell(\boldsymbol{r}_2)\Gamma_{ij,k\ell}\,d\boldsymbol{r}_2$$

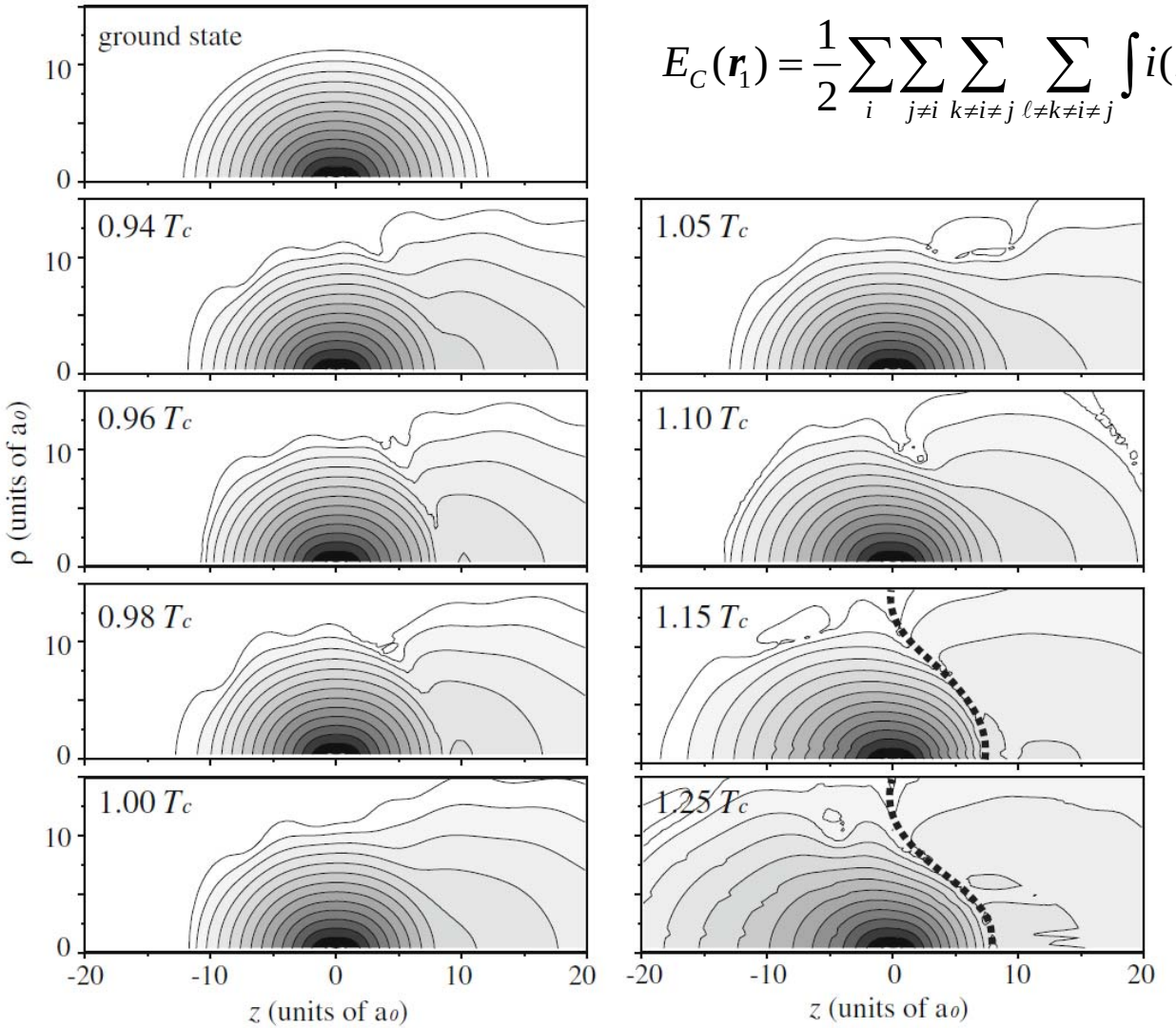

再散乱軌道の特定法

iとkの相関エネルギー

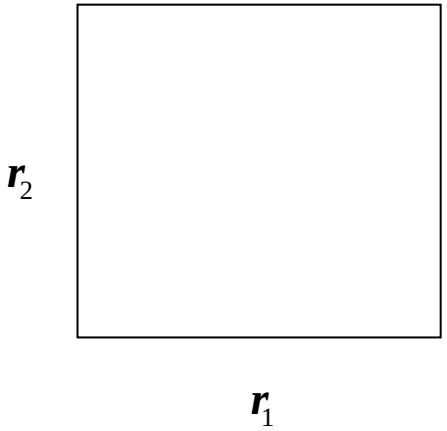

Fig. 2. Snapshots of the correlation energy density. The left-top panel shows the correlation energy density for the electronic ground state. The time for each panel is indicated in units of the laser optical cycle T_c. A logarithmic scale is employed for the modulus values from 10^{-2} to 10^{-15}. The broken lines drawn in the panels at $t = 1.15T_c$ and $1.25T_c$ show the zeros of the correlation density. In the two panels, the correlation density is positive in the right domain of the broken line while it is negative in the left domain.

Concluding Remarks

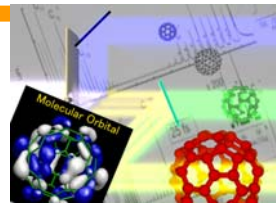

Analysis of the electronic dynamics
by using the “time-dependent” chemical potential

◆For stationary states or adiabatic processes:

The chemical potentials of natural orbitals are all degenerate.

◆Chemical potential vs. Energy supplied from the field

Small correlation energy ⇒ Spectator orbital (both are equal)

Energy exchange between natural orbitals through Correlation

⇒ Energy donating, accepting orbitals

Large increase in the chemical potential of a natural orbital ⇒ Ionization